Validation of a New Method for Finding the Rotational Axes of the Knee Using Both Marker-Based Roentgen Stereophotogrammetric Analysis and 3D Video-Based Motion Analysis for Kinematic Measurements

Michelle Roland
Department of Biomedical Engineering,
University of California,
One Shields Avenue,
Davis, CA 95616

M. L. Hull[1]
Department of Biomedical Engineering,
Department of Mechanical Engineering,
University of California,
One Shields Avenue,
Davis, CA 95616
e-mail: mlhull@ucdavis.edu

S. M. Howell
Department of Mechanical Engineering,
University of California,
One Shields Avenue,
Davis, CA 95616

In a previous paper, we reported the virtual axis finder, which is a new method for finding the rotational axes of the knee. The virtual axis finder was validated through simulations that were subject to limitations. Hence, the objective of the present study was to perform a mechanical validation with two measurement modalities: 3D video-based motion analysis and marker-based roentgen stereophotogrammetric analysis (RSA). A two rotational axis mechanism was developed, which simulated internal-external (or longitudinal) and flexion-extension (FE) rotations. The actual axes of rotation were known with respect to motion analysis and RSA markers within ±0.0006 deg and ±0.036 mm and ±0.0001 deg and ±0.016 mm, respectively. The orientation and position root mean squared errors for identifying the longitudinal rotation (LR) and FE axes with video-based motion analysis (0.26 deg, 0.28 m, 0.36 deg, and 0.25 mm, respectively) were smaller than with RSA (1.04 deg, 0.84 mm, 0.82 deg, and 0.32 mm, respectively). The random error or precision in the orientation and position was significantly better ($p = 0.01$ and $p = 0.02$, respectively) in identifying the LR axis with video-based motion analysis (0.23 deg and 0.24 mm) than with RSA (0.95 deg and 0.76 mm). There was no significant difference in the bias errors between measurement modalities. In comparing the mechanical validations to virtual validations, the virtual validations produced comparable errors to those of the mechanical validation. The only significant difference between the errors of the mechanical and virtual validations was the precision in the position of the LR axis while simulating video-based motion analysis (0.24 mm and 0.78 mm, $p = 0.019$). These results indicate that video-based motion analysis with the equipment used in this study is the superior measurement modality for use with the virtual axis finder but both measurement modalities produce satisfactory results. The lack of significant differences between validation techniques suggests that the virtual sensitivity analysis previously performed was appropriately modeled. Thus, the virtual axis finder can be applied with a thorough understanding of its errors in a variety of test conditions.
[DOI: 10.1115/1.4003437]

1 Introduction

Identifying the rotational axes of the tibio-femoral joint and modeling knee kinematics have been heavily studied in biomechanics literature because they aid in clinical diagnostics [1–4], help understand sport injury mechanisms [5,6], and are essential in developing new joint prosthetics and arthroplasties [3,7–9]. Several methods for identifying the rotational axes have been reported [10–12]; however, each has its limitations including position and orientation errors, which were unnecessarily large, mathematical derivations, which were not fully defined, and methods developed for coupled rotations in joints other than the knee. Recognizing these limitations motivated us to develop a new method called the virtual axis finder described in an earlier paper [12].

This virtual axis finder identifies the axis fixed in the femur about which the tibia flexes and extends, or the flexion-extension axis (FE axis) and the axis fixed in the tibia about which the tibia internally externally rotates, or the longitudinal rotational axis (LR axis), of the tibio-femoral joint by utilizing two mathematical optimizations, given kinematic data from pure internal-external rotation and natural flexion-extension. This process is done in two steps so that the coupled internal-external rotation that naturally occurs with flexion-extension can be mathematically eliminated when identifying the FE axis. The new method was validated virtually, with simulations of pure internal-external rotation and flexion-extension with coupled internal-external rotation. These simulations mimicked 3D video-based motion analysis as the kinematic measurement modality. The virtual validation included a sensitivity analysis, which assessed the sensitivity of the method

[1]Corresponding author.

Contributed by the Bioengineering Division of ASME for publication in the JOURNAL OF BIOMECHANICAL ENGINEERING. Manuscript received June 11, 2010; final manuscript received December 20, 2010; accepted manuscript posted January 14, 2011; published online April 11, 2011. Assoc. Editor: Richard Neptune.

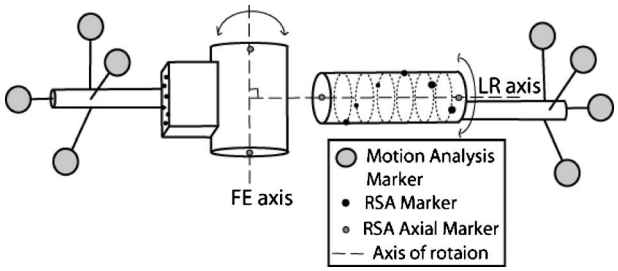

Fig. 1 Diagram of the two orientation axis mechanism. The horizontal shaft simulated the FE axis of rotation and the vertical axis simulated the LR axis of rotation. The axes of rotation were fixed with respect to one another so that they were perpendicular and intersecting. Six 0.8 mm diameter tantalum RSA markers were fixed to both shafts and two 0.8 mm diameter tantalum RSA axial markers were fixed along the geometric axes to identify the axes of rotation with respect to the RSA markers. An array of four reflective motion analysis markers was fixed to each shaft. A coordinate measurement machine was used to measure centroids of the reflective markers and the geometric axes of the shafts to identify the axes of rotation with respect to the motion analysis markers.

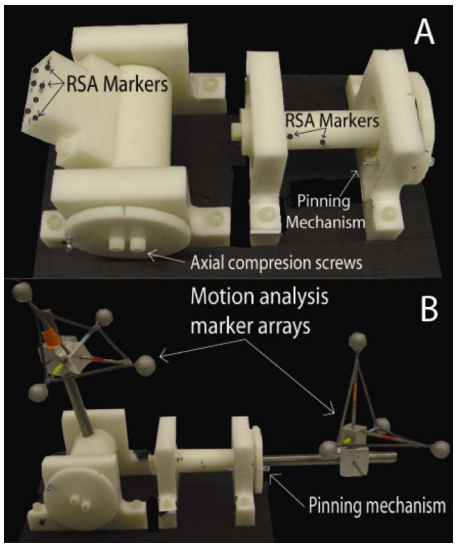

Fig. 2 Photographs of the two orientation axis mechanism with (*a*) RSA markers and (*b*) motion analysis markers. The shafts were rotated in 5 deg steps by rigidly pinning the large end disks to the pillow block by means of precision-machined holes placed in 5 deg steps along a 90 deg arc. The pillow blocks were mounted to a base plate to fix the orientation axes with respect to one another. The shafts rotated in ball bearings that were press fit into each pillow block. Axial compression along the inner race minimized off-axis motion.

to several factors that may differ between specimens and/or measurement modalities.

The validation and sensitivity analysis of the virtual axis finder indicated a substantial reduction in error when compared with the other methods available but several limitations motivate some additional development of the method. One is the lack of mechanical validation and the fact that the virtual validation simulated only one measurement modality (3D video-based motion analysis). Another is that the virtual simulated kinematic data represented optimal data collection techniques and some variables, such as orientation of the axes with respect to the virtual markers and the lack of any measurement bias, were simplified in the virtual model.

These limitations to the previously reported validation necessitate a thorough mechanical validation in which the virtual axis finder is put into practice with multiple kinematic measurement modalities. Thus, the primary objective was to quantify and compare the bias, precision, and root mean squared error (RMSE) of the virtual axis finder with a mechanical knee simulator between two kinematic measurement modalities, which can be used in vitro, bone mounted 3D video-based motion analysis and marker-based roentgen stereophotogrammetric analysis (RSA). As a secondary objective, the results of the mechanical validation were compared with virtual validations to assess the validity of the virtual simulations reported previously.

2 Methods

2.1 Two Rotational Axis Mechanism. To mechanically validate the virtual axis finder, a mechanism that could produce two pure rotational motions about known axes of rotation had to be utilized. Thus, we developed a two rotational axis mechanism that simulated tibio-femoral flexion-extension and internal-external rotational kinematics (Figs. 1 and 2). The mechanism allowed two rigid bodies to rotate independently about two fixed perpendicular axes of rotation [10,11]. The mechanism consisted of two shafts that were each supported by a pair of ball bearings and pillow blocks. To minimize off-axis motion of each shaft, we press fit the outer race of each ball bearing into custom made pillow blocks and the shafts were axially compressed against the inner race. The press fit and axial compression ensured that the axis of rotation for the shaft remained fixed with respect to the ball bearing and pillow block mechanism, which, therefore, allowed the geometrical axis of the shaft to remain collinear with the axis of rotation. To fix the two shafts with respect to one another, the two shafts and ball bearing pillow blocks were rigidly mounted to a base plate such that the axes of rotation were perpendicular and intersecting. Although the rotational axes may not be perpendicular and intersecting in practice, the relative position or orientation of the two rotational axes was examined virtually in pilot studies and no effect on the orientation and position errors in identifying the axes of rotation was observed. Precision-machined holes were placed on the pillow blocks in 5 deg increments about a 90 deg arc; this allowed the shafts to be rotated in 5 deg steps and pinned rigidly into place.

Because the objective was to simulate both marker-based RSA and 3D video-based motion analysis fixed to the bones, the two rotational axis mechanism was designed to be compatible with RSA tantalum markers as well as arrays of motion analysis reflective markers (Fig. 2). The position and orientation of both types of markers with respect to the axes of rotation were such that they simulated realistic placements in an actual tibio-femoral joint. Thus, the size, position, and orientation of the rotating shafts were selected to approximate the size and shape of a tibio-femoral joint truncated approximately 10–15 cm distal and proximal of the joint line. The longitudinal shaft simulated the tibia with six 0.8 mm tantalum markers fixed to the shaft such that they were equally spaced radially and axially about a 2.54 cm diameter and 10 cm length shaft, respectively. The horizontal shaft simulated the femur with six 0.8 mm tantalum markers fixed to a 5×8 cm^2 plane approximately 8 cm from and parallel to the horizontal axis of rotation. The six markers were placed approximately 1 cm from one another within that plane. Although it only requires three markers to track the position and orientation of each shaft, six markers were used to overdetermine the system and aid in reducing the measurement error [13]. An array of four 1.90 cm diameter reflective markers was fixed to a rod that was inserted axially but off-center, and distally into the longitudinal shaft. A second array of four 1.90 cm diameter reflective markers was fixed to a rod that was inserted perpendicularly and proximal to the horizontal axis of rotation (Fig. 1). The use of four-marker arrays overdetermined the system and aided in reducing the measurement error from motion analysis [13].

2.2 Gold Standard. To validate the virtual axis finder using the two rotational axis mechanism, the actual axes of rotation were identified with respect to the RSA markers and with respect to the motion analysis markers. For both cases, it was assumed that the geometric axes of the shafts were collinear with the axes about which the markers rotated. The axes were identified with marker-based RSA by fixing RSA axial markers directly on the geometric axis of the shafts. Using a lathe (± 0.0125 mm), 0.8 mm diameter holes were drilled approximately 2.5 mm deep along the geometric axis from both ends. The size of the drill bit was selected such that the 0.8 mm tantalum marker could be inserted into the hole with minimum pressure but could not slide in without an applied force. To ensure that the holes were placed precisely along the axis of the shafts, the axial alignment of the shafts with the drilling axis of the lathe was verified with a dial indicator to have less than 0.025 ± 0.0125 mm of off-axis travel over the 10 cm length of the shaft (less than 0.01 deg angular error). One 0.8 mm tantalum marker was fixed into each hole to mark two points on each axis of rotation. A Monte Carlo simulation was performed to estimate the precision in identifying the orientation and position of the actual axes of rotation with respect to the RSA markers. Normally distributed random variables with a zero mean and standard deviation (σ) were input into the simulation. The machining precision ($\sigma=0.025$ mm) and the measurement precision of RSA ($\sigma=0.05$ mm) were randomized with a normal distribution 1000 times and propagated through the calculations to identify the orientation and position errors of the actual axis with respect to the RSA markers. The output of the simulation estimated the precision of the orientation and position to be within ± 0.0006 deg and ± 0.036 mm, respectively.

The actual axes of rotation with respect to the motion analysis marker arrays were measured with a coordinate measurement machine (CMM) (Model SLCHM005L, Mitutoyo Corp., Aurora, IL). The centroid of each marker was identified with the sphere identification algorithm in the CMM software. A point on the axis of the shafts and the unit vector along the axis of the shafts were identified by the cylinder identification algorithm. The number of data points used for these algorithms was user defined to 15 and 30, respectively. Although the coordinate measurement machine has a 0.0001 mm precision, the irregularity of the reflective marker surfaces combined with the potential compliance of the arrays induced variability in identifying the centroids of the spheres and cylindrical axes. A truss system was added to each array to minimize the compliancy of the structure. To minimize the variability due to the irregularity of the marker surfaces, we increased the number of points used for each algorithm until the repeatability was equal to or less than 0.01 mm for the coordinates of each centroid and 0.0001 mm for the coordinates of the axial unit vector. A Monte Carlo simulation was performed to estimate the precision in identifying the orientation and position of the actual axes of rotation with respect to the motion analysis markers in a similar manner to the RSA simulations. The repeatability in measuring the centroids of the markers ($\sigma=0.01$ mm) and the unit vector along the axis of the shaft ($\sigma=0.0001$ mm) were randomized. The output of the simulation estimated the precision of the orientation and position to be within ± 0.0001 deg and ± 0.016 mm, respectively.

2.3 Testing. Global positions of the tantalum markers (± 0.05 mm) were obtained for each rotational step with biplanar radiographs taken of the two rotational axis mechanism while it was positioned inside the RSA calibration cube. To simulate pure internal-external rotation, the longitudinal shaft was rotated in 5 deg increments from 0 deg to 20 deg while the horizontal shaft remained fixed at 30 deg. For flexion-extension with coupled internal-external rotation, the horizontal shaft was rotated in 15 deg increments from 0 deg to 90 deg while the longitudinal shaft was rotated 15 deg during the first 30 deg of flexion. This process was repeated 5 times with the two rotational axis mechanism placed at various locations and orientations within the calibration cube to simulate five different specimens.

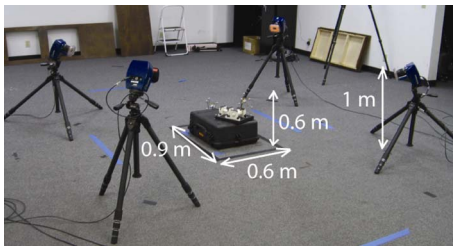

Fig. 3 Photograph of the video-based motion analysis set-up. The calibration volume was $0.6 \times 0.9 \times 0.6$ m^3 and the four Raptor 4 cameras (Motion Analysis Corp., Santa Rosa, CA) were positioned 1–1.3 m above the bottom of the calibrated volume in a 1.5 m arc around the center of the calibrated volume.

The motion analysis equipment and settings were utilized such that the tracking capabilities of the video cameras were optimized while maintaining a realistic laboratory setting for an in vitro study. Four 4.06 megapixel cameras (Raptor-4, Motion Analysis Corp., Santa Rosa, CA) were distributed evenly in a 1.5 m arc around a $0.6 \times 0.9 \times 0.6$ m^3 ($l \times w \times h$) calibrated volume. The cameras were vertically positioned between 1 m and 1.5 m above the base of the calibrated volume (Fig. 3). Data were collected in gray scale mode at 100 Hz for 5 s per rotational step in the same sequence used for the RSA testing. The process was repeated 5 times with the two rotational axis mechanism in varying positions and orientations within the calibrated volume to simulate five different specimens. Before each specimen's data sets began, it was verified that no significant marker occlusion existed for all four cameras for the given orientation and position of the mechanism. The position vectors of all eight markers were averaged over the 5 s data set for each rotational step and the average vectors were input into the virtual axis finding software. Thus, RSA and motion analysis had the same number of rotational steps and the same range of motion input into the software for optimization of the rotational axes.

2.4 Data Analysis. To optimize the position and orientation of the LR axis and the FE axis, the virtual axis finding software was utilized [12]. A marker coordinate system was defined and fixed to both the longitudinal (Tm) and horizontal (Fm) shafts. These coordinate systems were defined by three of the markers that were rigidly fixed to each shaft. To ensure that the constraint planes used to optimize the location of two points on each axis of rotation were approximately perpendicular to the axis of rotation, we had to transform the marker coordinate systems such that they were aligned with the axes of rotation. A pilot study was performed to ensure that deviating from this condition up to 5 deg and up to 5 mm does not affect the errors in this method. Thus, in practice, aligning the LR axis with the anatomic axis of the tibia and the FE axis with the transepicondylar axis of each coordinate system can create this transformation [10,11]. However, for this application, the marker coordinate systems Tm and Fm were transformed into axial coordinate systems Ta and Fa such that an axis in each of the axial coordinate systems was aligned with the LR axis and FE axis, respectively. Because the actual axes of rotation were collinear with one axis of their respective coordinate systems that were used to quantify the error, two projection angles fully described the error in orientation (Fig. 4). The position error was defined as the 2D position vector from the actual axes of rotation to the measured axes of rotation in a plane perpendicular to the actual LR ad FE axes. Because there is an infinite number of planes perpendicular to these axes, the plane with the smallest position vector magnitude was used to avoid compounding orien-

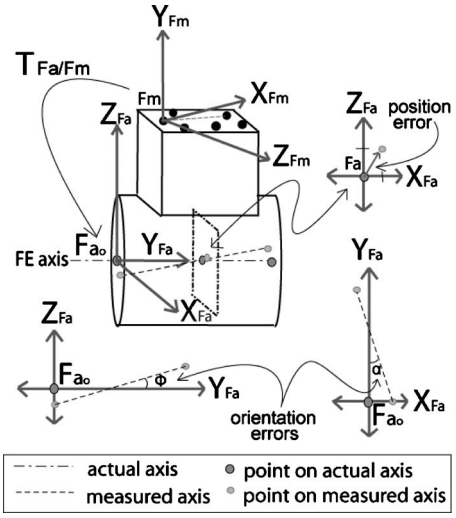

Fig. 4 Diagram of the transformations used to perform the error analysis with the FE axis shaft and RSA markers. The marker coordinate system (F_m), which was defined by three markers fixed to the shaft, is transformed into an axial coordinate system (F_a) such that one axis is aligned with the actual axis of rotation ($T_{Fa/Fm}$). The position error was defined by the 2D position vector from the FE axis to the measured axis in a plane that was perpendicular to the actual axis and contained the minimum distance between the actual and measured axes. The orientation error was defined by two projection angles (ϕ and α) between the measured and actual axes onto the two perpendicular planes that were parallel to the FE axis and contained the origin of the axial coordinate system (Z_{Fa}-Y_{Fa} and Y_{Fa}-X_{Fa} planes).

tation error into the position error. Thus, the error for each axis of rotation was described with four dependent variables: two orientation variables and two position variables (Fig. 4).

To quantify the accuracy of this method, we determined the bias defined as the average error, precision or random error defined as the standard deviation of the error, and RMSE over all five specimens and each dependent variable. The resulting error terms for the two projection angles were statistically pooled to provide the overall orientation error, and the two position variables were statistically pooled to provide the overall position error.

In the previous paper [12], a more thorough sensitivity analysis was performed in the virtual simulations; however, because these simulations were performed virtually, their applicability may be limited due to the assumptions and simplifications utilized in the virtual model. Thus, a comparison between the virtual validation and mechanical validation results was performed. Although the 3D video-based motion analysis virtual simulations were reported in the previous paper, certain aspects of that simulation did not correspond to the two rotational axis mechanism. Thus, the virtual validation was repeated such that marker positioning, measurement error, and positional error definitions aligned with the mechanical validation reported here. Virtual simulations of the marker-based RSA measurement modality were also performed as a second comparison of the two validation techniques. The RSA virtual model placed the markers in similar locations with respect to one another and to the axes as they were in the two rotational axis mechanism, and a measurement error of 0.05 mm [14] was incorporated into the virtual data. The virtual validations with motion analysis and RSA were each repeated 1000 times with rerandomized data to estimate the error accurately.

The variances between marker-based RSA and 3D video-based motion analysis for the orientation and position errors for the LR and FE axes were subjected to an F-test for variances (α=0.05) to determine whether there was a significant difference in the precision of identifying the axes between measurement modalities. Similarly, the variances between mechanical and virtual validations were subjected to an F-test (α=0.05) to determine whether there was a significant difference in the precision estimated from a mechanical validation versus a virtual validation. The mean error for each test was subjected to a student t-test (α=0.05) to determine whether there was a significant difference between measurement biases between measurement modalities as well as validation techniques. Independent two-sample t-tests for equal and unequal variances were utilized for each pair depending on the result of the F-test for equal variances. Finally, the mean squared error (MSE) ratio between RSA and motion analysis measurement modalities was subjected to an F-test to determine if there were significant differences between measurement modalities with the RMSE.

3 Results

The orientation and position errors for the LR and FE axes were considerably less with 3D video-based motion analysis than with marker-based RSA. The RMSEs in identifying the orientation and position of the LR axis with 3D video-based motion analysis were 0.26 deg and 0.28 mm, respectively, compared with 1.04 deg and 0.84 mm, respectively, with marker-based RSA. The orientation and position RMSE were 75% and 67% less with motion analysis than with RSA (Fig. 5), which was a significant difference (p =0.01 and p=0.03, respectively). Likewise, the RMSEs in identi-

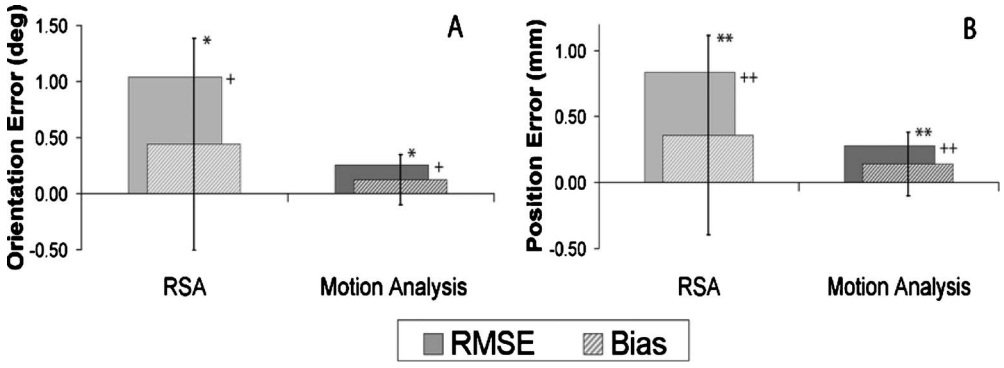

Fig. 5 Bar chart comparing marker-based RSA and 3D video-based motion analysis as the measurement modality for the (*a*) orientation and (*b*) position RMSE, bias, and precision (error bars) for identifying the LR axis of rotation. There was a significant difference between precisions for the orientation (*p=0.008) and the position (**p=0.024) errors and a significant difference between RMSE for the orientation (+p=0.01) and position (++p=0.03) errors.

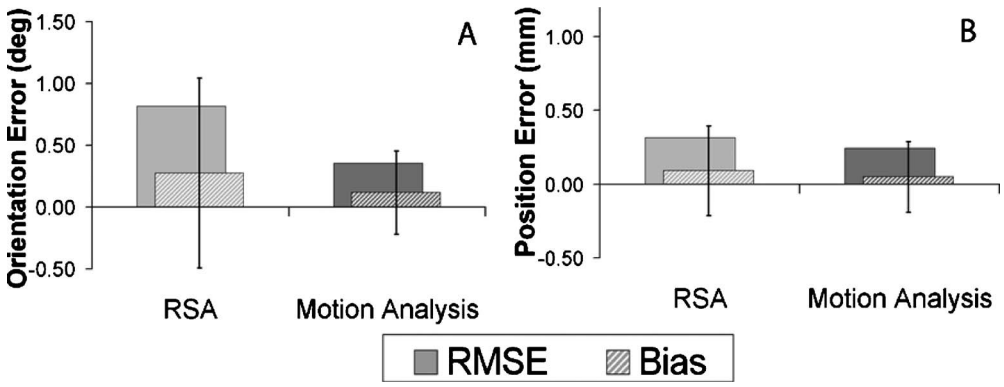

Fig. 6 Bar chart comparing marker-based RSA and 3D video-based motion analysis as the measurement modality for the (*a*) orientation and (*b*) position RMSE, bias, and precision (error bars) for identifying the FE axis of rotation. There was no significant difference.

fying the orientation and position of the FE axis with 3D video-based motion analysis were 0.36 deg and 0.25 mm, respectively, compared with 0.82 deg and 0.32 mm, respectively, with RSA. The 56% decrease in orientation and 23% decrease in position RMSE with motion analysis compared with RSA with the FE axis was not significant ($p=0.22$ and $p=0.41$, respectively) (Fig. 6).

There was significantly more variability (i.e., less precision) in identifying the orientation ($p=0.008$) and position ($p=0.024$) of the LR axis with marker-based RSA (0.95 deg and 0.76 mm) than with 3D video-based motion analysis (0.23 deg and 0.24 mm) (Fig. 5). However, there was no significant difference between variances for the FE axis ($p=0.07$). Also, there was no significant difference between bias errors for either the LR or FE axes ($p=0.51$).

In comparing the virtual validation to the mechanical validation, in general, the errors compared closely for both 3D video-based motion analysis (Table 1) and marker-based RSA (Table 2). There was a significant difference between variances for the position errors ($p=0.019$) on the LR axis with motion analysis simulations; however, there was no other significant difference between validation techniques. The bias errors for the mechanical validations were nonzero, whereas the bias errors for the virtual validation were negligible.

4 Discussion

Identifying the rotational axes of the tibio-femoral joint and modeling knee kinematics have been heavily studied in biomechanics literature, and the accuracy of these models have been shown to have a significant impact on their applicability. Limitations to previously reported methods to identify the rotational axes of the tibio-femoral joint prompted us to develop the virtual axis finder described in a previous paper [12]. However, there were several limitations to the virtual validation that necessitated a thorough mechanical validation in which the virtual axis finder was put into practice with multiple kinematic measurement modalities.

Table 1 Average errors in identifying the LR and FE axes of rotation with a mechanical validation versus a virtual validation for video-based motion analysis. The virtual validations mimicked the mechanical validations with marker placement, rotational axis placement, and measurement error. Mechanical validations had an n of 5 and virtual validations had an n of 1000. The asterisks denote a significant difference between mechanical and virtual validation techniques ($p=0.019$).

	LR axis				FE axis			
	Orientation (deg)		Position (mm)		Orientation (deg)		Position (mm)	
	Mech.	Virtual	Mech.	Virtual	Mech.	Virtual	Mech.	Virtual
Bias	0.10	0.00	0.10	0.00	0.12	0.01	0.05	0.01
Precision	0.23	0.27	0.24*	0.78*	0.34	0.41	0.24	0.25
RMSE	0.25	0.27	0.26	0.78	0.36	0.41	0.25	0.25

Table 2 Average errors in identifying the LR and FE axes of rotation with a mechanical validation versus a virtual validation for marker-based RSA. The virtual validations mimicked the mechanical validations with marker placement, rotational axis placement, and measurement error. Mechanical validations had an n of 5 and virtual validations had an n of 1000.

	LR axis				FE axis			
	Orientation (deg)		Position (mm)		Orientation (deg)		Position (mm)	
	Mech.	Virtual	Mech.	Virtual	Mech.	Virtual	Mech.	Virtual
Bias	0.27	0.00	0.12	0.03	0.28	0.03	0.09	0.03
Precision	0.95	1.22	0.76	0.50	0.77	0.83	0.30	0.37
RMSE	0.98	1.22	0.77	0.50	0.82	0.83	0.32	0.37

Thus, our primary objective of this work was to validate mechanically the virtual axis finder with marker-based RSA and video-based motion analysis. A secondary objective was to compare the results of the mechanical validation to the virtual validations to verify the applicability of the previously reported virtual validation. The virtual axis finder successfully identified the LR and FE axes of rotation using both marker-based RSA and 3D video-based motion analysis as the measurement modalities. However, the errors for orientation and position of the LR and FE axes were reduced with motion analysis compared with RSA (Figs. 5 and 6). A second key finding was that the validation performed with virtually created data produced higher errors than the validation performed with the two rotational axis mechanism. However, the difference in the precision of identifying the position of the LR axis while simulating motion analysis was the only dependent variable that was significantly different between validation techniques.

Although marker-based RSA and 3D video-based motion analysis are common kinematic measurement modalities in tibiofemoral biomechanics research, there are several other techniques used in this field that were not studied here. For example, the instrumented spatial linkage (ISL) [15–17] and model-based RSA [18,19] using fluoroscopy are two modalities that might be used to provide the kinematic data necessary as input to the virtual axis finder. Because of the errors unique to each of these measurement modalities, it would be advisable to validate the modality of interest using a mechanical validation such as that described herein.

The fact that the precision in identifying the LR axis was significantly better with video-based motion analysis than with marker-based RSA can be explained by two variables: the difference in measurement errors between the two measurement modalities and the use of multiple data points per rotational step with motion analysis. Although the exact measurement error of the motion analysis system used herein has not been reported, another four-camera Vicon system of similar capabilities was reported to have an overall measurement bias of 63 ± 5 μm and a measurement precision of 15 μm [14] in comparison to marker-based RSA, which has negligible measurement bias and a measurement precision of 49 μm [20]. Furthermore, because marker-based RSA utilized just one set of radiographs at each rotational step, only one datum sample was available. On the other hand, video-based motion analysis data were collected at 60 Hz over 5 s, providing 300 data samples per rotational step. Thus, utilizing the average result from a set of data provided improved measurement precision of the motion analysis data.

It is important to note that although the measurement precision of our data within a given rotational step was 6 μm, which was comparable to the values reported with the Vicon system mentioned above, an imprecision in the distance between markers on the two arrays when the orientation of the arrays was changed was observed to be 150 μm. This imprecision was likely due to partial occlusions of the markers from the truss system built into the arrays for rigidity. Although this phenomenon did not have a large impact on the capabilities of the virtual axis finder, as evidenced by the results reported here, this phenomenon should be taken into consideration when designing motion analysis arrays in practice.

Because the virtual errors were consistently larger than the mechanical validation errors and because there were few significant differences between the mechanical and virtual validation techniques, it can be concluded that the virtual simulations appropriately modeled each measurement modality. This result provides evidence that the virtually based sensitivity analysis reported previously is an accurate representation of the errors that can be expected in practice in the absence of skin movement artifacts. Furthermore, those results are, if anything, slightly overestimating the errors.

An important assumption in this validation for video-based motion analysis as the measurement modality was the absence of skin motion artifact. It is our intention to use this method in a cadaveric study in which the marker arrays are fixed to the bones, thus eliminating skin motion artifact from this measurement modality. The application of this modality in vivo would undoubtedly introduce skin motion errors and deviate from the conditions tested here; therefore, this modality should not be used with in vivo applications without further development to address these errors. However, because the measurement errors innate to marker-based RSA are not affected by in vivo applications, RSA could be used when this method is applied in vivo.

The quasi-static measurements used in this method pose another potential limitation to the application of the virtual axis finder with video-based motion analysis. Because measurements were taken at static rotational steps through the range of motion, the random measurement errors innate to 3D video-based motion analysis were partially filtered out. It is probable that without filtering the measurement errors in this manner, the virtual axis finder will not exhibit or identify the axes of rotation with the same error [12].

Another limitation with both the virtual and mechanical validation techniques was that the marker coordinate systems were fixed to the rotating bodies such that they were intentionally aligned to the actual axes of rotation. This was done to simplify the modeling and to provide anatomically relevant results. However, this was considered to be a potential source of error in practice because perfect alignment will not be possible. Thus, pilot studies were performed with the mechanical data in which the marker coordinate systems were translated and rotated from the actual axes of rotation. There was no change to either the bias or precision errors of the virtual axis finder during these pilot studies; therefore, this independent variable and the attendant errors were not included in the analysis reported here.

The results of these validations indicate that 3D video-based motion analysis using four Raptor 4 cameras is a better measurement modality than marker-based RSA for use with the virtual axis finder; however, both methods provided satisfactory results. Given these results, the virtual axis finder maintains a large scope of applicability in the biomechanics field, as suggested in the previous paper. Furthermore, because the virtual validation tends to overestimate the error when compared with the mechanical validation, the sensitivity analysis reported previously estimates the upper end of the error scale with this method. Thus, this method can be utilized with a thorough understanding of the expected errors under a variety of test conditions and applications.

Acknowledgment

We are grateful to Motion Analysis Corporation and particularly Dustin Hatfield for assisting with the data collection using their system.

References

[1] Hicks, J., Arnold, A., Anderson, F., Schwartz, M., and Delp, S., 2007, "The Effect of Excessive Tibial Torsion on the Capacity of Muscles to Extend the Hip and Knee During Single-Limb Stance," Gait and Posture, **26**, pp. 546–552.

[2] Van Gheluwe, B., Kirby, K. A., and Hagman, F., 2005, "Effects of Simulated Genu Valgum and Genu Varum on Ground Reaction Forces and Subtalar Joint Function During Gait," J. Am. Podiatr. Med. Assoc., **95**, pp. 531–541.

[3] Fuchs, B., Kotajarvi, B. R., Kaufman, K. R., and Sim, F. H., 2003, "Functional Outcome of Patients With Rotationplasty About the Knee," Clin. Orthop. Relat. Res., **415**, pp. 52–58.

[4] Reinbolt, J. A., Haftka, R. T., Chmielewski, T. L., and Fregly, B. J., 2008, "A Computational Framework to Predict Post-Treatment Outcome for Gait-Related Disorders," Med. Eng. Phys., **30**, pp. 434–443.

[5] Besier, T. F., Lloyd, D. G., Ackland, T. R., and Cochrane, J. L., 2001, "Anticipatory Effects on Knee Joint Loading During Running and Cutting Maneuvers," Med. Sci. Sports Exercise, **33**, pp. 1176–1181.

[6] Besier, T. F., Lloyd, D. G., Cochrane, J. L., and Ackland, T. R., 2001, "External Loading of the Knee Joint During Running and Cutting Maneuvers," Med. Sci. Sports Exercise, **33**, pp. 1168–1175.

[7] Asano, T., Akagi, M., and Nakamura, T., 2005, "The Functional Flexion-Extension Axis of the Knee Corresponds to the Surgical Epicondylar Axis: In Vivo Analysis Using a Biplanar Image-Matching Technique," J. Arthroplasty, **20**, pp. 1060–1067.

[8] Edwards, M. L., 2000, "Below Knee Prosthetic Socket Designs and Suspension Systems," Physical Medicine and Rehabilitation Clinics of North America, **11**, pp. 585–593.
[9] Incavo, S. J., Coughlin, K. M., Pappas, C., and Beynnon, B. D., 2003, "Anatomic Rotational Relationships of the Proximal Tibia, Distal Femur, and Patella: Implications for Rotational Alignment in Total Knee Arthroplasty," J. Arthroplasty, **18**, pp. 643–648.
[10] Hollister, A. M., Jatana, S., Singh, A. K., Sullivan, W. W., and Lupichuk, A. G., 1993, "The Axes of Rotation of the Knee," Clin. Orthop. Relat. Res., **290**, pp. 259–268.
[11] Churchill, D. L., Incavo, S. J., Johnson, C. C., and Beynnon, B. D., 1998, "The Transepicondylar Axis Approximates the Optimal Flexion Axis of the Knee," Clin. Orthop. Relat. Res., **356**, pp. 111–118.
[12] Roland, M. R., Hull, M. L., and Howell, S. M., 2010, "Virtual Axis Finder: A New Method to Determine the Two Kinematic Axes of Rotation for the Tibio-Femoral Joint," ASME J. Biomech. Eng., **132**, p. 011009.
[13] Woltring, H. J., 1994, "3-D Attitude Representation of Human Joints: A Standardization Proposal," J. Biomech., **27**, pp. 1399–1414.
[14] Windolf, M., Gotzen, N., and Morlock, M., 2008, "Systematic Accuracy and Precision Analysis of Video Motion Capturing Systems—Exemplified on the Vicon-460 System," J. Biomech., **41**, pp. 2776–2780.
[15] Lewis, J. L., Lew, W. D., and Schmidt, J., 1988, "Description and Error Evaluation of an In Vitro Knee Joint Testing System," ASME J. Biomech. Eng., **110**, pp. 238–248.
[16] Kirstukas, S. J., Lewis, J. L., and Erdman, A. G., 1992, "6R Instrumented Spatial Linkages for Anatomical Joint Motion Measurement—Part 1: Design," ASME J. Biomech. Eng., **114**, pp. 92–100.
[17] Ishii, Y., Terajima, K., Koga, Y., and Bechtold, J. E., 1999, "Screw Home Motion After Total Knee Replacement," Clin. Orthop. Relat. Res., **358**, pp. 181–187.
[18] Hoff, W. A., Komistek, R. D., Dennis, D. A., Gabriel, S. M., and Walker, S. A., 1998, "Three-Dimensional Determination of Femoral-Tibial Contact Positions Under In Vivo Conditions Using Fluoroscopy," Clin. Biomech. (Bristol, Avon), **13**, pp. 455–472.
[19] Hanson, G. R., Suggs, J. F., Freiberg, A. A., Durbhakula, S., and Li, G., 2006, "Investigation of In Vivo 6 DOF Total Knee Arthoplasty Kinematics Using a Dual Orthogonal Fluoroscopic System," J. Orthop. Res., **24**, pp. 974–981.
[20] Roos, P., Hull, M. L., and Howell, S. M., 2004, "How Cyclic Loading Affects the Migration of Radio-Opaque Markers Attached to Tendon Grafts Using a New Method: A Study Using Roentgen Stereophotogrammetric Analysis RSA," J. Biomech., **126**, pp. 62–69.